Antagonistic Regulation of Native Ca^{2+}- and ATP-sensitive Cation Channels in Brain Capillaries by Nucleotides and Decavanadate

László Csanády and Vera Adam-Vizi

Department of Medical Biochemistry, Semmelweis University, and Neurochemical Group of the Hungarian Academy of Sciences, Budapest H-1444, Hungary

ABSTRACT Regulation by cytosolic nucleotides of Ca^{2+}- and ATP-sensitive nonselective cation channels (CA-NSCs) in rat brain capillary endothelial cells was studied in excised inside-out patches. Open probability (P_o) was suppressed by cytosolic nucleotides with apparent K_I values of 17, 9, and 2 μM for ATP, ADP, and AMP, as a consequence of high-affinity inhibition of channel opening rate and low-affinity stimulation of closing rate. Cytosolic [Ca^{2+}] and voltage affected inhibition of P_o, but not of opening rate, by ATP, suggesting that the conformation of the nucleotide binding site is influenced only by the state of the channel gate, not by that of the Ca^{2+} and voltage sensors. ATP inhibition was unaltered by channel rundown. Nucleotide structure affected inhibitory potency that was little sensitive to base substitutions, but was greatly diminished by 3′-5′ cyclization, removal of all phosphates, or complete omission of the base. In contrast, decavanadate potently ($K_{1/2}$ = 90 nM) and robustly stimulated P_o, and functionally competed with inhibitory nucleotides. From kinetic analyses we conclude that (a) ATP, ADP, and AMP bind to a common site; (b) inhibition by nucleotides occurs through simple reversible binding, as a consequence of tighter binding to the closed-channel relative to the open-channel conformation; (c) the conformation of the nucleotide binding site is not directly modulated by Ca^{2+} and voltage; (d) the differences in inhibitory potency of ATP, ADP, and AMP reflect their different affinities for the closed channel; and (e) though decavanadate is the only example found to date of a compound that stimulates P_o with high affinity even in the presence of millimolar nucleotides, apparently by competing for the nucleotide binding site, a comparable mechanism might allow CA-NSC channels to open in living cells despite physiological levels of nucleotides. Decavanadate now provides a valuable tool for studying native CA-NSC channels and for screening cloned channels.

KEY WORDS: microscopic reversibility • competitive binding • kinetic model • Trp channels • blood-brain-barrier

INTRODUCTION

Ca^{2+}- and ATP-sensitive nonselective cation channels (CA-NSCs) are present in various tissues, such as acinar (Maruyama and Petersen, 1982; Suzuki and Petersen, 1988) and ductal (Gray and Argent, 1990) cells of the exocrine pancreas, kidney (Paulais and Teulon, 1989), brain endothelium (Popp and Gögelein, 1992), brown adipose tissue (Koivisto et al., 2000), cultured rat cardiac cells (Colquhoun et al., 1981; Guinamard et al., 2002), vomeronasal sensory neurons (Liman, 2003), and astrocytes (Chen and Simard, 2001). For many other nonselective cation channels that have been found in native tissues (Marty et al., 1984; Gögelein and Capek, 1990), as well as in some endothelial (Kamouchi et al., 1999; Suh et al., 2002) and nonendothelial (Yellen, 1982; Sturgess et al., 1986; Jung et al., 1992) cell lines, inhibition by direct application of nucleotides in inside-out patches has not yet been studied. Although suggested to belong to the Trp family of ion channels (Petersen, 2002), the molecular identity of CA-NSC channels is not yet certain. These channels can be activated by Ca^{2+} from the cytosolic side (Ca^{2+}_i) in excised patches (Popp and Gögelein, 1992; Csanády and Adam-Vizi, 2003) or through stimulation of various cell-surface receptors that increase Ca^{2+}_i in intact cells (Maruyama and Petersen, 1982; Kamouchi et al., 1999; Koivisto et al., 2000). Differing sensitivity profiles for inhibition by micromolar cytosolic nucleotides have been described for CA-NSC channels in astrocytes (Chen and Simard, 2001), in brown fat cells (Halonen and Nedergaard, 2002), and in the kidney (Paulais and Teulon, 1989), as well as in an insulinoma cell line (Sturgess et al., 1986), but the mechanism of this inhibition has not yet been elucidated.

In a previous study we have examined the regulation by Ca^{2+} and voltage of the CA-NSC channels present in rat brain capillary endothelial cells (Csanády and Adam-Vizi, 2003), and the present work was aimed at clarifying the mechanism of regulation by nucleotides.

If micromolar concentrations of cytosolic nucleotides do indeed inhibit CA-NSC channels, it remains unclear

The online version of this article contains supplemental material.

Address correspondence to László Csanády, Department of Medical Biochemistry, Semmelweis University, 1444 Budapest, Pf. 262., Hungary. Fax: (36) 1-267-0031; email: csanady@puskin.sote.hu

Abbreviations used in this paper: CA-NSC, Ca^{2+}- and ATP-sensitive nonselective cation channel; DV, decavanadate.

J. Gen. Physiol. © The Rockefeller University Press • 0022-1295/2004/06/743/15 $8.00
Volume 123 June 2004 743–757
http://www.jgp.org/cgi/doi/10.1085/jgp.200309008

how they could become activated, as reported, in intact cells, in which nucleotide concentrations are generally in the millimolar range. ATP-sensitive K^+ channels are also inhibited by binding of micromolar cytosolic ATP to the pore-forming subunit, but this inhibition is counteracted by channel stimulation through binding of cytosolic MgADP to the regulatory sulphonylurea receptor subunit (Tucker and Ashcroft, 1998). In contrast, most CA-NSC channels are inhibited not only by cytosolic ATP, but also by ADP and AMP (Sturgess et al., 1986; Paulais and Teulon, 1989; Halonen and Nedergaard, 2002), raising the question of how the reported strong inhibition by nucleotides is counteracted in living cells to allow the channels to open.

Using inside-out patches excised from rat brain capillary endothelial cells we have examined in detail the effect on CA-NSC gating of cytosolic ATP, ADP, AMP, as well as a number of other nucleotides. Our results suggest that all of these nucleotides share a common binding site on the CA-NSC channel, and that inhibition occurs through simple reversible binding that leads to a stabilized closed state in which the nucleotide is more tightly bound. Furthermore, we find that decavanadate (DV) can counteract nucleotide inhibition, apparently by binding competitively to the same site. Robust stimulation of CA-NSC channels by decavanadate, even in the presence of millimolar nucleotide, is a consequence of its extremely high (nanomolar) affinity for the open-channel conformation. An as yet unknown putative activator molecule might act through a similar mechanism to permit CA-NSC function in intact cells.

MATERIALS AND METHODS

Preparation and Culture of Rat Brain Capillary Endothelial Cells

Primary cultures of rat brain capillary endothelial cells were prepared as described (Dömötör et al., 1998) by isolating microvessels from rat brain by gradient centrifugation. Collagenase/dispase–digested capillaries were seeded on glass coverslips precoated with a biological matrix, and nonendothelial cells were selectively killed by complement-mediated lysis. Recordings were made after 5–6 d of culture.

Calibration of Decavanadate Concentrations

DV stock solution was prepared by adjusting the pH of a 50 mM Na_3VO_4 solution to 2.0, at which pH DV is the major vanadium species (Csermely et al., 1985). This stock was stored at +4°C and used within 24 h for dilution into the bath freshly (<90 min) before each experiment. The rate of decay of DV in our bath solution (pH = 7.1, T = 25°C) was measured by photometry (Varga et al., 1985) as peak absorption at ~390 nm (against a blank with identical composition, but boiled; see Fig. 4), and actual concentrations were calculated accordingly for each experiment.

Excised-patch Recording

Excised, inside-out patch recordings were performed at 25°C using an Axopatch 200B amplifier and Pclamp 8 software for data acquisition (Csanády and Adam-Vizi, 2003). Currents were filtered at 1 kHz with a 4-pole Bessel filter and digitally sampled at 5 kHz. Pipette (extracellular) solution contained (in mM) 140 NaCl, 2 $MgCl_2$, 1 $CaCl_2$, 10 HEPES, and 30 μM benzamil (pH = 7.4). The continuously flowing bath (intracellular) solution contained (in mM) 140 KCl, 2 $MgCl_2$, 10 HEPES (pH = 7.1). Because CA-NSC channels rapidly lose their sensitivity for Ca^{2+} after patch excision (Csanády and Adam-Vizi, 2003), channels were reversibly activated by adding 1 mM $CaCl_2$ to the bath solution (bars in Figs. 1 and 4–6), except in Fig. 2, A and C, where ATP-inhibition was tested in the presence of 10 mM and 100 μM Ca^{2+}, respectively. Nucleotides (Sigma-Aldrich) were diluted into the bath from pH-adjusted aqueous stock solutions, and free Ca^{2+} and Mg^{2+} was kept constant by adding appropriate amounts of $CaCl_2$ and $MgCl_2$ (calculated by WinMaxc). Except for Fig. 2 B, pipette holding potential was +40 mV (V_m = −40 mV). CA-NSC channels, identified by their obligatory dependence on cytosolic Ca^{2+} for opening, as well as by their nucleotide sensitivity, were responsible for all unitary channel openings we could observe under the above conditions, since the other two possible sources of inward unitary Na^+ current in our cells, stretch-activated channels and amiloride-sensitive cation channels, were eliminated by the absence of stretch and by pipette benzamil, respectively (Csanády and Adam-Vizi, 2003).

Kinetic Analysis

Kinetic analysis was done using custom-written software. Current records were digitally filtered with a 200-Hz Gaussian filter, slow baseline-drifts removed using a baseline-update algorithm sensitive to single-channel current transitions (Csanády et al., 2000). Baseline-subtracted currents were idealized using half-amplitude threshold crossing with a fixed dead time of 1 ms (Csanády, 2000).

Dwell-time histograms of single CA-NSC channels are complex even in the absence of nucleotides, due to complex regulation by Ca^{2+} and voltage (Csanády and Adam-Vizi, 2003). In the absence of a reliable scheme to describe Ca^{2+}- and voltage-dependent gating on its own, mechanistic interpretation of nucleotide-mediated changes in the dwell-time distributions is not feasible at present. On the other hand, most of the data presented here were recorded from patches with multiple (1–10) active channels to obtain sufficient numbers of events even under strong inhibition by nucleotides. Therefore, kinetic parameters were not extracted from traditional fitting of dwell-time histograms. Instead, P_o, opening and closing rates were obtained using the cycle-time method (Csanády and Adam-Vizi, 2003). Open probability (P_o) was calculated from the events lists as $\Sigma_k(n_k t_k)/(NT)$, where n_k and t_k denote the number of open channels and the duration, respectively, of the kth event, N is the number of channels in the patch, and $T = \Sigma_k t_k$ is the total duration of the record. (The number of channels (N) was taken as the maximum number of simultaneously open channels observed immediately upon excision into 1 mM Ca^{2+} when P_o was close to unity.) Mean open time (*m.o.t.*) and mean closed time (*m.c.t.*), i.e., the arithmetic average of the open and closed dwell times of a single channel, were calculated as *m.o.t.* = $\Sigma_k(n_k t_k)/$(number of upward transitions), and *m.c.t.* = (*m.o.t.*)$((1/P_o) - 1)$. Average opening rate was then defined as $1/$*m.c.t.*, and closing rate as $1/$*m.o.t.*

Experiments were performed by applying test concentrations of nucleotides or DV bracketed by control segments recorded in the absence of ligand. Normalized P_o, opening and closing rates (in Figs. 1, 2, 5, 6, and 8) were obtained by normalizing the kinetic parameter in the presence of ligand to the average of that parameter in the bracketing control segments.

Individual normalized dose response curves in Figs. 1, 2, and 5–7 were fit, using a nonlinear least-squares fitter (SigmaPlot 8.0), by Hill-functions of the form

$$Y([S]) = Y(\infty)\frac{[S]^n}{[S]^n + K_{1/2}^n} + Y(0)\frac{K_{1/2}^n}{[S]^n + K_{1/2}^n}, \quad (1)$$

where $[S]$ denotes the concentration of ligand, $K_{1/2}$ is the half-maximally effective ligand concentration, and n is the Hill-coefficient (and $Y(0)$ was fixed to 1). Fitted $K_{1/2}$ values are printed in the figure panels, and n values are given in the figure legends.

Ensemble fitting of all dose response curves (Fig. 8) by various models was done by custom-written software. To calculate the error function, the differences between the predicted parameters (see equations for each model in online supplemental material, sections 2.1–2.6) and the measured values of normalized P_o, opening and closing rate were squared and summed for all conditions (18 dose response curves, several ligand concentrations each). (Errors for closing rates in the presence of nucleotides were weighted by 1/20 to compensate for the fact that these curves were normalized to their minimum values; see Fig. 1 D.) Because at steady-state the ligand binding/unbinding steps influence channel opening rates, closing rates, and P_o only through their equilibrium constants (K_ds), not through the absolute values of on- and off-rate, only K_ds were fitted for these transitions (e.g., "horizontal" transitions in the schemes shown in Fig. 1 E and Fig. 8). The error function was then minimized with respect to the kinetic constants involved, using a downhill simplex algorithm (Caceci and Cacheris, 1984).

Single-channel Conductances

All-points histograms of segments of current recordings, obtained at membrane potentials between −80 and +80 mV, were fitted with sums of Gaussians, and distances between adjacent peaks were plotted against voltage, to obtain current-voltage (i/V) plots. For the Na^+/K^+ condition (Na^+ in the pipette, K^+ in the bath), with or without DV, channel conductances and reversal potentials were obtained from straight-line fits to each plot. For the $Na^+/NMDG^+$ condition, with or without DV, i/V plots were fitted to the Goldmann-Hodgkin-Katz current equation written for two permeant ions,

$$i_{fit}(V) = \quad (2)$$

$$\gamma \cdot V \cdot \left(\frac{p_{NMDG}}{p_{Na}} z_{NMDG}^2 \frac{[NMDG^+]_o - [NMDG^+]_i \cdot e^{z_{NMDG}FV/(RT)}}{1 - e^{z_{NMDG}FV/(RT)}} + z_{Na}^2 \frac{[Na^+]_o - [Na^+]_i \cdot e^{z_{Na}FV/(RT)}}{1 - e^{z_{Na}FV/(RT)}} \right),$$

to obtain parameters (p_{NMDG}/p_{Na}) and γ [pS/mM] (p_X and z_X, permeability and valence of ion X^+). Reversal potentials were obtained by solving $i_{fit}(V) = 0$ and conductances were defined as the asymptotic slopes of the fits at very negative potentials (where, from the above equation, $g_- = \gamma [Na^+]_o$).

Statistics

Unless otherwise indicated, all data points in the figures represent the averages of at least five measurements, and error bars are SEM.

Online Supplemental Material

Mathematical details of some of the analyses used in this paper are available at http://www.jgp.org/cgi/content/full/jgp.200309008/DC1. Section 1 of this supplemental material provides the mathematical proof that the loop-criterion for microscopic reversibility can be applied to average rates among compound states. Section 2 contains the derivations of the equations that describe open probabilities (and opening and closing rates for the scheme in Fig. 1 E) as a function of various ligand concentrations for all of the kinetic schemes considered. Subsection 2.1 deals with the basic scheme in Fig. 1 E, subsections 2.2–2.6 discuss five different possible ways of extending that model to include two different ligands. Section 3 discusses the results of fitting the five extended models to the ensemble of the data, as illustrated in Fig. S1. All sections are referenced by section number at the appropriate locations in the main text.

RESULTS

Micromolar Cytosolic Nucleotides Inhibit CA-NSC Channels by Slowing Opening Rate and Speeding Closing Rate

CA-NSC channels activated by cytosolic Ca^{2+} in inside-out patches from brain endothelial cells promptly and reversibly close upon superfusion with millimolar cytosolic ATP (Popp and Gögelein, 1992; Csanády and Adam-Vizi, 2003). We found a similar inhibition of open probability (P_o) when we superfused our patches with ATP, ADP or AMP (Fig. 1 A); fits to the Hill-equation (Eq. 1, MATERIALS AND METHODS) yielded apparent $K_{1/2}$ values of 17 ± 1, 9.4 ± 1, and 2.4 ± 0.2 μM, respectively (Fig. 1 B, solid lines). This suggests that inhibition is not dependent on ATP hydrolysis. Kinetic analysis showed that all three nucleotides inhibited P_o by slowing channel opening (Fig. 1 C) and speeding closure (Fig. 1 D). Interestingly, $K_{1/2}$ (from fits to the Hill-equation; Fig. 1 C, solid lines) for inhibition of opening rate was ~2-fold lower in each case than for inhibition of P_o (11 ± 2, 4.3 ± 0.5, and 1.1 ± 0.2 μM for ATP, ADP, and AMP), whereas closing rates were stimulated only at higher cytosolic nucleotide concentrations, and failed to saturate even in the 100-micromolar range. (The plots in Fig. 1 D could not be reliably fitted with the Hill equation since closing rates failed to saturate even in the presence of millimolar nucleotide, while low opening rates precluded collection of events at even higher concentrations.)

These findings can be rationalized by a simple model (Fig. 1 E) in which nucleotides bind both to the closed and the open channel. According to the thermodynamic principle of microscopic reversibility, for a closed kinetic scheme the product of the rates around a loop is identical in both directions. Because nucleotide binding stabilizes the closed state of the CA-NSC channel, to maintain reversibility, the nucleotide must be bound more tightly in the closed than in the open state. For the scheme in Fig. 1 E, $K_{1/2}$ for opening rate (Fig. 1 C) equals the dissociation constant (K_d) of the nucleotide from the closed channel, while $K_{1/2}$ for closing rate (compare, Fig. 1 D) reflects the K_d of the open channel (see online supplemental material, section 2.1, Eqs. 9 and 10). Therefore, the large separation between

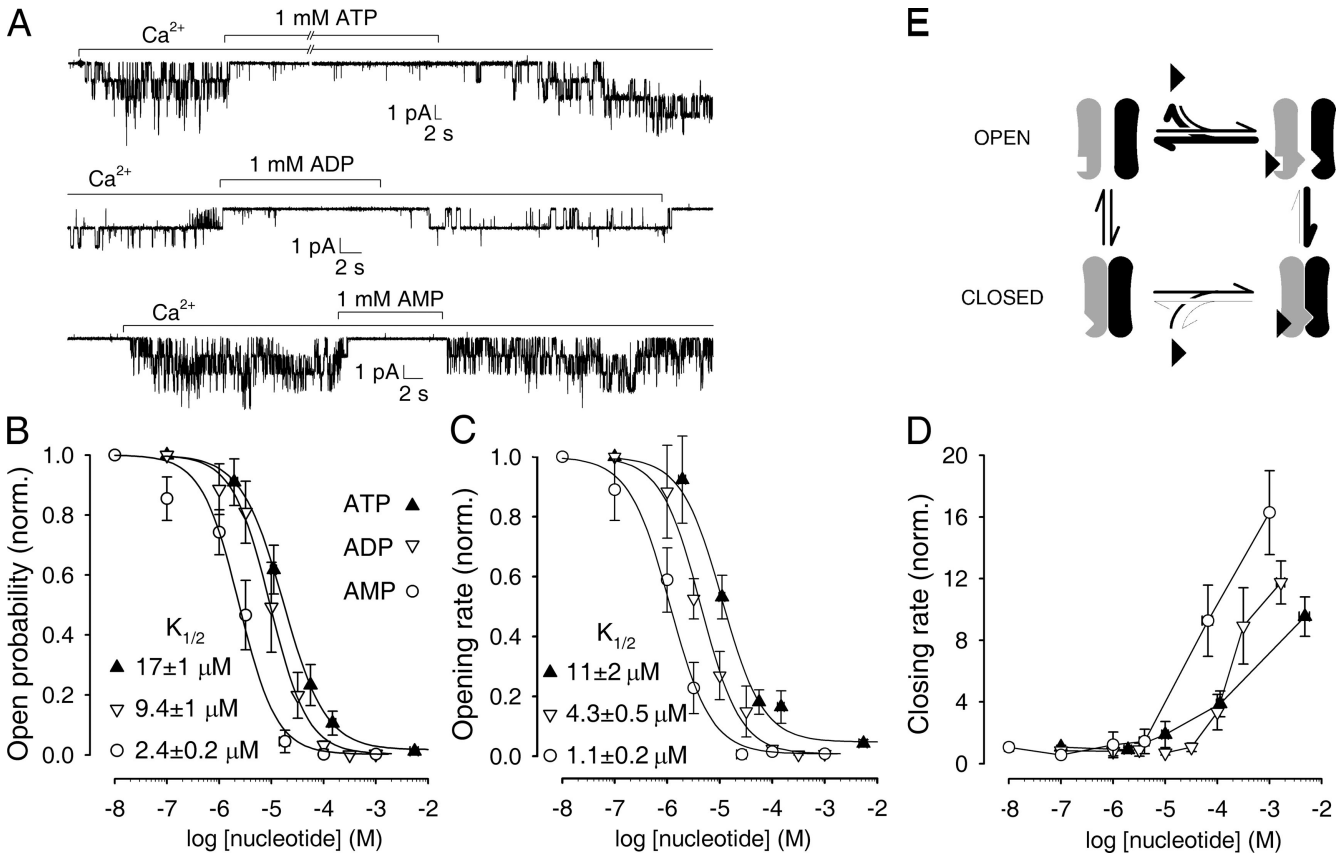

FIGURE 1. Inhibition of CA-NSC channel gating by ATP, ADP, and AMP. (A) Current traces from patches superfused with 1 mM cytosolic nucleotide during activation by 1 mM Ca^{2+} (bars). (B–D) P_o (B), opening (C), and closing rates (D) as a function of nucleotide concentrations, normalized to control values in the absence of nucleotide (see MATERIALS AND METHODS). Solid lines in B and C are fits to the Hill equation (Eq. 1, MATERIALS AND METHODS), midpoints ($K_{1/2}$) are printed in each panel. Hill constants (n) were 1.1 ± 0.03, 1.2 ± 0.1, and 1.2 ± 0.2 for P_o and 1.1 ± 0.2, 1.2 ± 0.1, and 1.1 ± 0.1 for opening rate in ATP, ADP, and AMP. The leftmost data point in B–D (and Figs. 2 and 5–8) represents control. (E) Simple model of reversible nucleotide binding.

the efficiencies of nucleotides for affecting opening vs. closing rate is consistent with our simple scheme.

Inhibition by Nucleotides Is Not Affected by Channel Rundown

CA-NSC channels from brain capillaries are opened by micromolar cytosolic $[Ca^{2+}]$ ($[Ca^{2+}]_i$), but after patch excision they rapidly (within 30–60 s) deactivate ("run down"); ~1 min after excision millimolar Ca^{2+} is required for channel opening (Csanády and Adam-Vizi, 2003). To detect any parallel changes in nucleotide sensitivity, we performed experiments in which test concentrations of ATP were briefly applied immediately after patch excision into a bath containing 100 μM free Ca^{2+}. CA-NSC channels were initially opened to a P_o of close to unity in 100 μM Ca^{2+} (Fig. 2 A, patch with 6 channels); superfusion with ATP, only ~10 s after excision, resulted in prompt inhibition of channel activity. Quantitation of such experiments was hampered by rapid rundown (note, only two of the six channels were still recovered with high Ca^{2+} affinity after the brief, ~12-s exposure to ATP, Fig. 2 A). Nevertheless, a tentative analysis of gating parameters in ATP, normalized to the bracketing segments, yielded dose response curves of P_o, opening and closing rates (Fig. 2, D–F, open circles) qualitatively similar to those obtained for deactivated channels at steady-state in 1 mM Ca^{2+} (open triangles, replotted from Fig. 1, B–D, for comparison). In particular, inhibition of P_o resulted from high-affinity inhibition of opening rate and low-affinity stimulation of closing rate, with fits to the Hill equation (dotted lines) yielding $K_{1/2}$ values of 34 ± 3, and 15 ± 2 μM, respectively, for P_o and opening rate. Because rundown had no great influence on nucleotide inhibition (especially considering opening rate, see also below), and because the time window before deactivation was too narrow, we restricted the present study on nucleotide inhibition to partially deactivated CA-NSC channels gating steadily in 1 mM $[Ca^{2+}]_i$ (Figs. 1–8, except for Fig. 2, A and B, below).

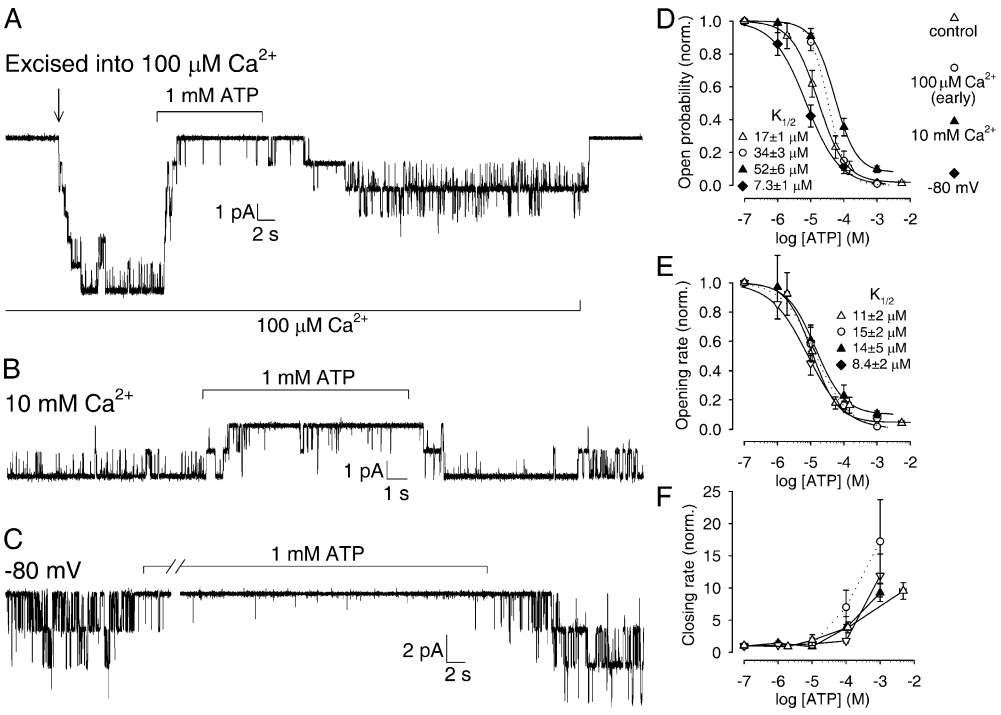

FIGURE 2. Influence of channel rundown, $[Ca^{2+}]_i$, and voltage on ATP inhibition. (A) Excision of a patch containing six CA-NSC channels into a bath with 100 μM Ca^{2+} maximally activates all six channels; brief application of 1 mM cytosolic ATP (bar) ~10 s after excision promptly inhibits channel activity. Note, incomplete recovery of channel activity after ATP exposure due to rapid rundown. (B and C) Current traces from patches (minutes after excision) superfused with 1 mM cytosolic ATP (bar) during exposure to either 10 mM Ca^{2+} (at −40 mV, B), or to 1 mM Ca^{2+} at −80 mV (C). The patch in B contained two, the one in C at least five active channels. (D–F) Normalized P_o (D), opening (E), and closing rates (F) as a function of [ATP] for the conditions described in A (open circles), B (solid triangles), and C (solid diamonds) compared with control condition in 1 mM Ca^{2+}_i at −40 mV (open triangles, replotted from Fig. 1, B–D). Solid lines (and dotted line, for the condition in A) in D, E, and F are fits to the Hill equation (Eq. 1, MATERIALS AND METHODS); midpoints ($K_{1/2}$) are printed in each panel. Hill constants (n) were 1.6 ± 0.1, 1.3 ± 0.2, and 0.9 ± 0.1 for P_o and 0.9 ± 0.1, 1.0 ± 0.3, and 0.8 ± 0.1 for opening rate for conditions A, B, and C, respectively.

Inhibition of Open Probability, but Not of Opening Rate, by Nucleotides Is Sensitive to [Ca^{2+}] and Voltage

Because the equilibrium between open and closed states of the CA-NSC channel (i.e., vertical transitions in Fig. 1 E) is regulated by $[Ca^{2+}]_i$ and voltage (Csanády and Adam-Vizi, 2003), we tested how these parameters affect nucleotide inhibition.

Raising $[Ca^{2+}]_i$ from 1 to 10 mM stimulated partially deactivated CA-NSC channels from a typical P_o of 0.4–0.5 to a P_o of close to unity (Fig. 2 B; Csanády and Adam-Vizi, 2003). Under such conditions cytosolic ATP still inhibited (Fig. 2 B), but the dose response curve for inhibition of P_o was shifted to the right (Fig. 2 D, solid triangles); the $K_{1/2}$ value obtained from a Hill-fit (solid line) was 52 ± 6 μM. Conversely, when the membrane potential (V_m) was hyperpolarized from −40 mV (used throughout this study) to −80 mV (all in 1 mM Ca^{2+}_i), P_o typically decreased to ~0.2 (Fig. 2 C; Csanády and Adam-Vizi, 2003). ATP inhibited P_o at −80 mV (Fig. 2 C) slightly more potently than at −40 mV; a Hill-fit to the dose response curve (Fig. 2 D, solid diamonds) yielded a $K_{1/2}$ of 7.3 ± 1 μM (solid fit line).

Under both of these altered conditions, ATP inhibition of P_o resulted from inhibition of opening rate (Fig. 2 E) together with stimulation of closing rate (Fig. 2 F). In both cases inhibition of opening rate occurred with high affinity while stimulation of closing rate required high concentrations of ATP with no saturation apparent at 1 mM. These results further corroborate the scheme put forward in Fig. 1 E. Interestingly, while [Ca^{2+}] and voltage shifted the apparent affinity for ATP as reflected by P_o (Fig. 2 D), no such effect was apparent in the dose response curves for inhibition of opening rate (Fig. 2 E). Hill-fits (solid lines) yielded $K_{1/2}$ values for opening rate of 14 ± 5 and 8.4 ± 2 μM, respectively, in 10 mM Ca^{2+} (−40 mV) and at −80 mV (1 mM Ca^{2+}), none of which differed significantly from the control value obtained at −40 mV in 1 mM Ca^{2+} (11 ± 2 μM, Fig. 2 E, open triangles and solid line).

ATP Inhibition Is a Function of Total [ATP], Rather Than of Free [ATP]

Because altering free [Ca^{2+}] alters the fractional distribution of ATP among its free (ATP^{4-}, free ATP) and divalent-bound (Ca-ATP, Mg-ATP) forms, we tested whether the ATP-binding site on the CA-NSC channel selectively binds any one of these ATP species. As inhibition of P_o is a complicated function of several parameters, including control P_o in the absence of ATP (online supplemental material, section 2.1., Eq. 12, available at http://www.jgp.org/cgi/content/full/jgp.200309008/DC1; see also DISCUSSION below), a

TABLE I

Effect of Divalent-bound, Free, and Total [ATP] on Channel Opening Rate

Condition		Opening rate (normalized)	$[ATP_{total}]$	[Mg-ATP][a]	[Ca-ATP][a]	[free ATP][a]
			μM	μM	μM	μM
(a)	100 μM free Ca^{2+},[b] 2 mM free Mg^{2+}	0.58 ± 0.11 (n = 5)	10	9.29	0.41	0.30
(b)	1 mM free Ca^{2+}, 2 mM free Mg^{2+}	0.62 ± 0.12 (n = 3)	10	6.83	2.95	0.22
(c)	10 mM free Ca^{2+}, 2.01 mM free Mg^{2+}	0.61 ± 0.10 (n = 4)	10	1.87	8.07	0.06
(d)	1 mM free Ca^{2+}, 0.184 mM free Mg^{2+}	0.094 ± 0.043 (n = 6)	100	16.41	77.74	5.85
(e)	1 mM free Ca^{2+}, 2.03 mM free Mg^{2+}	0.10 ± 0.03 (n = 14)	100	68.55	29.24	2.21
(f)	1 mM free Ca^{2+}, 9.91 mM free Mg^{2+}	0.16 ± 0.06 (n = 6)	100	91.38	8.02	0.60

Opening rates were normalized to that measured under the same ionic conditions (same free $[Ca^{2+}]$ and $[Mg^{2+}]$) in the absence of ATP. Total $[Ca^{2+}]$, $[Mg^{2+}]$, and [ATP] for conditions a–e were as follows (in mM): 0.10, 2.01, 0.01 for a; 1.0, 2.01, 0.01 for b; 10.0, 2.01, 0.01 for c; 1.08, 0.20, 0.10 for d; 1.03, 2.10, 0.10 for e; and 1.01, 10.0, 0.10 for f, respectively.

[a]Calculated using Winmaxc (pH = 7.1, T = 25°C).

[b]Tested immediately after excision.

more reliable parameter for assessing nucleotide binding affinity is inhibition of opening rate (or closing rate; however, we could not obtain complete dose response curves for the latter); from the scheme in Fig. 1 E, $K_{1/2}$ for opening rate is equal to the K_d of ATP from the closed channel (online supplemental material, section 2.1., Eq. 9).

We therefore measured opening rates under various free $[Ca^{2+}]$ and $[Mg^{2+}]$ and either 10 or 100 μM total [ATP], and normalized these rates to those obtained in bracketing control segments under identical ionic conditions (same free $[Ca^{2+}]$ and $[Mg^{2+}]$) but no ATP. Table I summarizes normalized opening rates, and lists total [ATP], as well as [Mg-ATP], [Ca-ATP], and [free-ATP] calculated using the freeware program Winmaxc. Inhibition of opening rate was similar in all three cases where total [ATP] was 10 μM (conditions a–c in Table I), while [Mg-ATP] varied over an ∼5-fold, [Ca-ATP] over an ∼20-fold, and [free-ATP] over an ∼5-fold range. Likewise, 100 μM total [ATP] caused similar inhibition of opening rate (conditions d–f in Table I), while [Mg-ATP] varied by ∼6-fold, [Ca-ATP] by ∼10-fold, and [free-ATP] by ∼10-fold. These results cannot be explained by selective binding of any of the three ATP species; rather, they indicate that the ATP binding site of the CA-NSC channel does not greatly discriminate, at least between Ca-ATP and Mg-ATP. We cannot rule out that free ATP does not bind at all, since this species represents a negligible fraction of total [ATP] (<6%) under all conditions tested, and CA-NSC channels cannot be studied in divalent-free solutions where free ATP would be the predominant species.

Distinct Profile of Nucleotide Inhibitory Potency for Brain Endothelial CA-NSC Channels

We examined how inhibition depends on the structural elements of the nucleotide (Fig. 3, A and C). The poorly hydrolyzable ATP analogue AMPPNP effectively inhibited, further supporting the above conclusion that simple binding of ATP, not hydrolysis of its γ-phosphate, was required. Substitutions of the adenine ring by guanine (GTP) or uracil (UTP) were compatible with inhibition, in contrast to complete removal of the base (ribose-5P) or its replacement with a negatively charged phosphate group (phospho-ribosyl-PP). Although AMP was the most potent inhibitor (Fig. 1), its 3′-5′ cyclic form cAMP failed to affect gating, as did cGMP. High-affinity inhibition required the presence

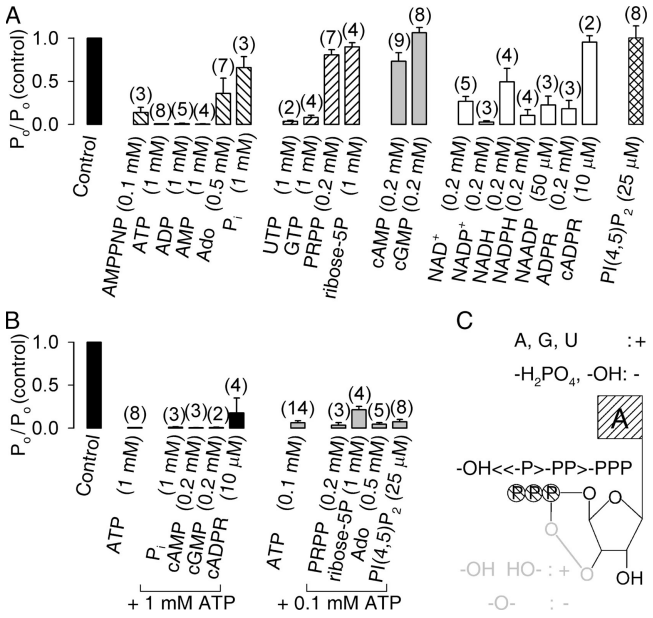

FIGURE 3. Profile of inhibition by various nucleotides. (A) Inhibition of P_o, relative to control, by cytosolic exposure at indicated concentrations to nucleotides with various numbers of phosphates (▨), base substitutions (▨), or cyclic structure (■), to dinucleotides (□), and to $PI(4,5)P_2$ (☒). (B) Nucleotides which fail to inhibit P_o, cannot prevent inhibition by concomitantly added ATP. (C) Sketch summary of structural requirements for inhibition.

of at least one phosphate, as adenosine (Ado) inhibited only at high concentrations. Inorganic phosphate (P_i) alone had little effect (but 2 mM pyrophosphate caused 92 ± 2% inhibition (n = 4)). While high concentrations of dinucleotides like NAD^+, $NADP^+$, NADH, NADPH, NAADP, and ADP-ribose (but not cADP-ribose) inhibited to a variable extent, we cannot rule out the possibility of a slight contamination of our dinucleotide stocks by AMP. Importantly, none of the above compounds that failed to inhibit channel activity (e.g., P_i, cAMP, cGMP, cADP-ribose, Ado, ribose-5P, PRPP) could prevent inhibition by concomitantly added ATP (Fig. 3 B), suggesting that these compounds failed to inhibit gating because they did not bind to the channels. Thus, as summarized in the sketch in Fig. 3 C, inhibitory potency requires a purine or pyrimidine base and one or more phosphate groups (with one phosphate being optimal) without 3′-5′ cyclization.

Although a lipid, not a nucleotide, phosphatidyl inositol 4,5-bisphosphate ($PI(4,5)P_2$) is known to modulate a variety of cation channels, including several Trp channels (Liu and Liman, 2003; Prescott and Julius, 2003), as well as ATP-sensitive K^+ channels (Loussouarn et al., 2001; Rohacs et al., 2003), where it competes off inhibitory ATP (MacGregor et al., 2002). We therefore tested a short-chain (dioctanoyl), water-soluble, form of $PI(4,5)P_2$, which, however, affected neither CA-NSC gating (Fig. 3 A) nor inhibition by 100 μM ATP (Fig. 3 B).

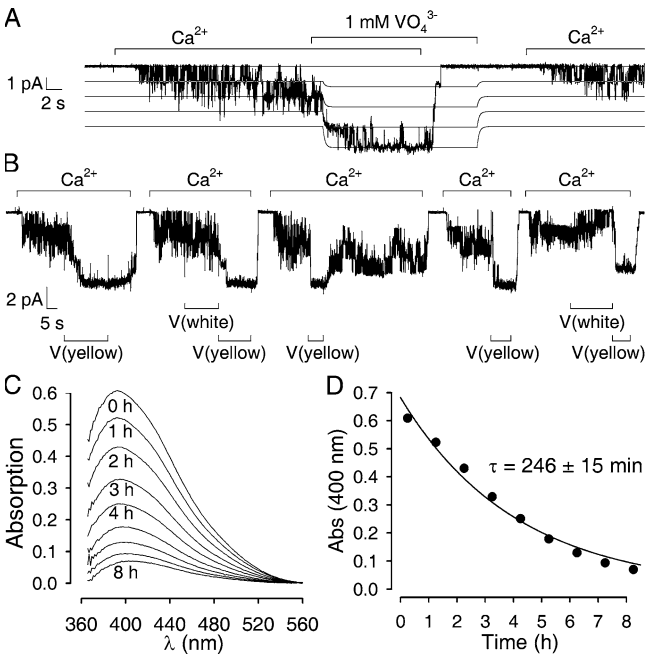

FIGURE 4. Cytosolic DV reversibly stimulates CA-NSC channel currents. (A) Addition of 1 mM Na_3VO_4 to the bath (bar) reversibly increases both P_o and single-channel current size (gray lines); patch with four channels. (B) Effects on CA-NSC channel activity of DV-free (boiled, colorless) and untreated (slightly yellow) vanadate solution in a patch containing four channels. (C) Absorption spectra of an untreated 1 mM Na_3VO_4 solution (pH = 7.1, T = 25°C) 0–8 h after preparation. [DV] is monitored as peak absorption at ∼390 nm. (D) Decay time course of DV at pH = 7.1, T = 25°C, and single-exponential fit.

Decavanadate Is a Potent Activator of CA-NSC Channels That Stimulates P_o with Nanomolar Affinity

While P_i was without effect, when we perfused our channels with a 1-mM solution of the P_i-analogue orthovanadate, we saw, to our surprise, robust stimulation of channel gating to a P_o close to unity, together with a clear (∼30%) increase in single-channel current size (Fig. 4 A); however, activity remained Ca^{2+} dependent as witnessed by prompt closure of all channels when Ca^{2+} was washed off in the continued presence of vanadate. When millimolar crystalline orthovanadate is dissolved at neutral pH, trace amounts of its decamer (DV) inevitably form, causing the appearance of a faint yellow color. DV-free, colorless, vanadate solution can be prepared, e.g., by boiling (Csermely et al., 1985). Such DV-free vanadate solutions were without effect on CA-NSC gating, while, in the same patches, the control (yellow) vanadate solution repeatedly produced maximal stimulation (Fig. 4 B), suggesting that DV, and not orthovanadate, was responsible for the effect. To verify this idea, and to quantitate the amount of DV in our bath solution, we prepared a stable DV stock solution (pH = 2, see MATERIALS AND METHODS), from which we diluted fresh DV into our bath solution immediately before each experiment. [DV] of our bath solution was monitored with a spectrophotometer as absorption at ∼390 nm (Fig. 4 C). Repeated photometry showed that DV decayed with a time constant of ∼4 h in this solution (pH = 7.1, T = 25°C) (Fig. 4 D). Actual [DV] was therefore calculated for each experiment by correcting for the decay expected from the time lag between the dilution of DV and the experiment itself.

Recordings in a range of cytosolic [DV] showed stimulation of channel P_o already at nanomolar [DV], at which concentrations no effect on channel conductance was apparent (Fig. 5 A). P_o was stimulated with a $K_{1/2}$ of 90 ± 16 nM (Fig. 5 B), mainly due to slowed channel closure (Fig. 5 C), together with a slight increase in average opening rate (Fig. 5 D).

Stimulation of Gating by Decavanadate and Inhibition of Gating by Nucleotides are Functionally Competitive Effects

Interestingly, DV not only robustly stimulated gating, but could also prevent inhibition by concomitantly added ATP, ADP, or AMP. Thus, in the presence of ∼8 μM DV (∼90× its own $K_{1/2}$, see Fig. 5 B) channel gating was maximally stimulated, and remained insensitive

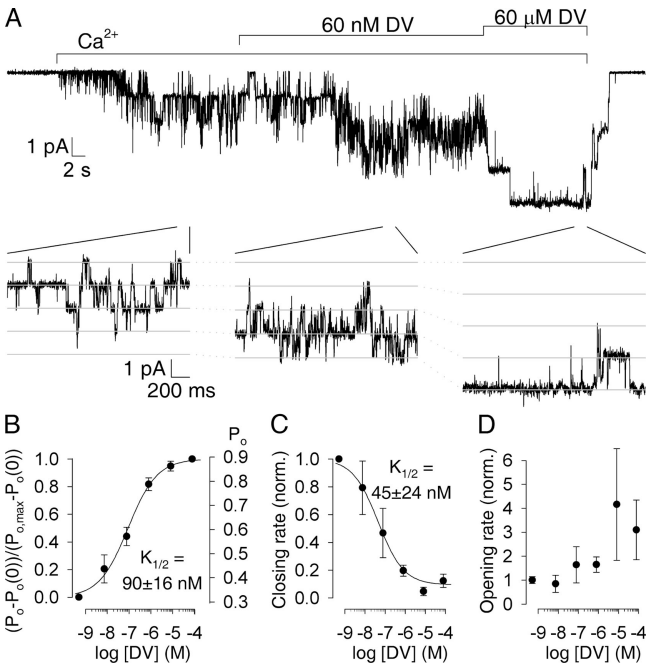

FIGURE 5. Stimulation of gating by nanomolar concentrations of DV. (A) Currents from a patch with four CA-NSC channels recorded in response to superfusion with increasing [DV]. Inset with expanded time scale allows visual inspection of gating versus permeation effects. (B–D) Normalized P_o (B), closing (C), and opening rates (D) as a function of [DV]. Solid lines in B and C are fits to the Hill equation (Eq. 1, MATERIALS AND METHODS), midpoints ($K_{1/2}$) are printed in each panel, $n = 0.7 \pm 0.1$ (B) and 0.7 ± 0.2 (C).

to superfusion with 1 or 10 μM AMP; even in 1 mM AMP P_o remained ~0.25, 10 mM AMP being needed for near-complete inhibition (Fig. 6 A). $K_{1/2}$ for inhibition by AMP was increased ~90× (to 232 ± 51 μM, Fig. 6 B), as would be expected for a simple competitive mechanism, i.e., DV and AMP competing for a single binding site (see online supplemental material, section 2.2, Eq. 14b). Similarly, ~1.6 μM DV (~20× its own $K_{1/2}$) increased $K_{1/2}$ for inhibition by ADP and ATP ~20× (to 215 ± 33 μM, Fig. 6 C) and ~40× (to 677 ± 159 μM, Fig. 6 D), respectively. Conversely, AMP could prevent stimulation by DV. When the effect on gating of increasing [DV] was assessed in the presence of constant 1 mM AMP (~400× its own $K_{1/2}$), 24 ± 5 μM DV was required for half-maximal stimulation, ~270× more than under control conditions (Fig. 6, E and F). Similarly, ADP and ATP at a concentration of 1 mM, ~100×, and ~50× higher than their own $K_{1/2}$ values, increased $K_{1/2}$ for DV by ~80× (to 7.4 ± 1 μM, Fig. 6 G) and ~35× (to 3.0 ± 1 μM, Fig. 6 H), respectively.

Micromolar Decavanadate Enhances Single-channel Conductance Irrespective of the Presence of Nucleotides

Single-channel current amplitudes were increased in all recordings where DV was present (Figs. 4–6). We recorded gating at various membrane voltages in the presence of a maximally effective [DV] of 70 μM, and constructed single-channel current-voltage (*i(V)*) curves (Fig. 7 A). With NaCl in the pipette and KCl in the bath the *i(V)* curve remained linear in the presence of DV, and the slope conductance increased by 34 ± 2% ($n = 9$) relative to control (from 30 ± 1 pS to 42 ± 3 pS) without a measurable change in reversal potential (from −3 ± 2 mV to −1 ± 2 mV). When the impermeant cation $NMDG^+$ replaced K^+ in the bath, 70 μM DV caused slightly larger inward currents while, just as without DV, no outward current could be resolved; asymptotic conductances at negative potentials (defined in MATERIALS AND METHODS, see Eq. 2) increased from 32 ± 3 pS ($n = 3$) to 36 ± 0.5 pS ($n = 3$). This effect on conductance of the pore was apparent only at micromolar [DV] (Figs. 5 A and 7 B) with a $K_{1/2}$ of 1.7 ± 0.3 μM (Fig. 7 C), ~20-fold higher than $K_{1/2}$ for stimulation of gating (Fig. 5 B). Furthermore, simultaneously added nucleotides that efficiently competed off the gating effect of DV did not reverse the increase in single-channel current size (Fig. 7 B, also Fig. 6, A and E). In addition, the *i([DV])* dose response curve was not altered by 1 mM ATP, ADP, or AMP (Fig. 7 C), nor could we detect any systematic change in conductance upon addition of nucleotides, regardless of the presence or absence of DV (Fig. 7 D).

DISCUSSION

Inhibition by Nucleotides Is an Intrinsic Property of CA-NSC Channels

CA-NSC channels freshly excised from brain endothelial cells are activated by micromolar Ca^{2+} (compare Fig. 2 A), with a $[Ca^{2+}]_i$ of ~20 μM required for half-maximal activation (Csanády and Adam-Vizi, 2003), similar to that reported in excised patches for large conductance Ca^{2+}-activated K^+ (Pérez et al., 2001), TrpM4b (Nilius et al., 2003), and TrpM5 (Hofmann et al., 2003; Liu and Liman, 2003) channels (although higher Ca^{2+} affinities were concluded for the latter two in some whole-cell studies; Launay et al., 2002; Prawitt et al., 2003). Within ~1 min of excision, Ca^{2+} affinity of our CA-NSC channels declines such that channel activation requires millimolar Ca^{2+}_i (Csanády and Adam-Vizi, 2003). The cause of this loss of sensitivity toward activating Ca^{2+} is incompletely understood. Because Ca^{2+} dependence is dramatically altered by this run-down phenomenon, and because our detailed steady-state studies on nucleotide inhibition were done minutes after excision, we verified whether CA-NSC channels could be inhibited by ATP freshly after excision, in their presumably more "native-like" state. Our experiments confirmed ATP inhibition of freshly excised channels with characteristics similar to those of deacti-

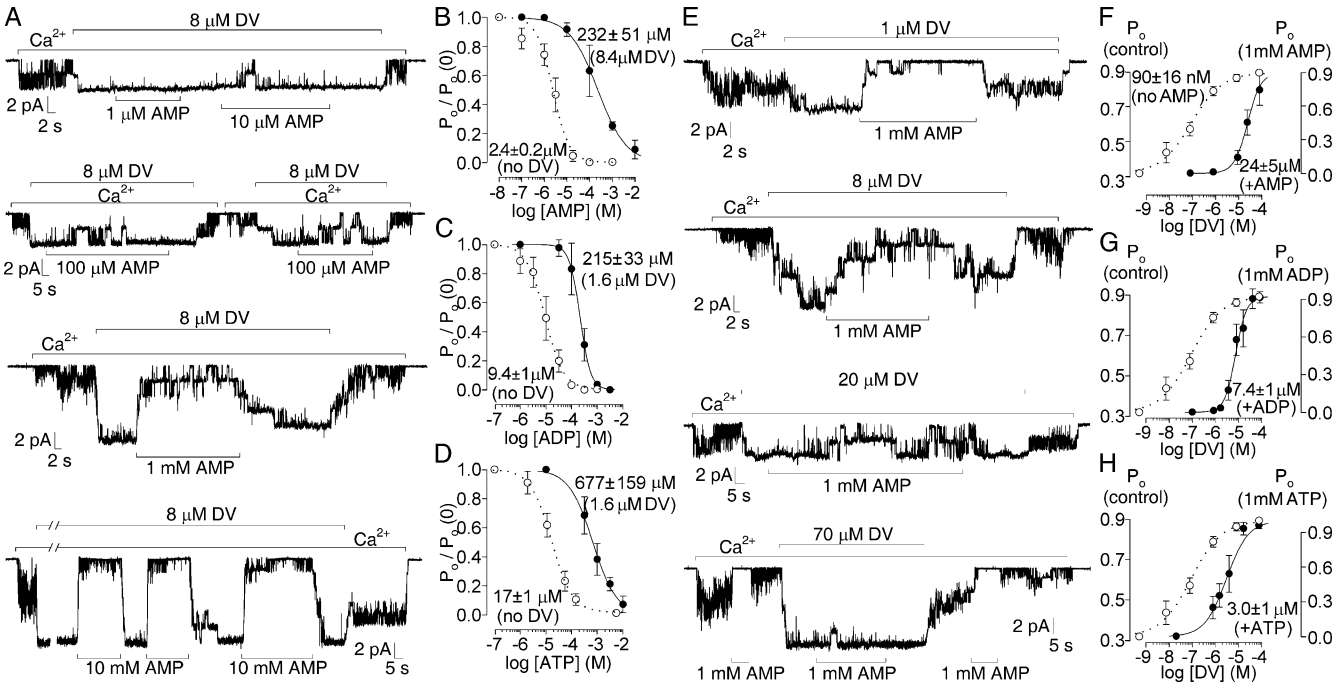

FIGURE 6. DV and nucleotides shift each others affinity for affecting gating. (A and E) Current traces showing incremental inhibition of gating by 1, 10, 100 μM, and 1 and 10 mM AMP, all in ~8 μM DV (A), and incremental stimulation of gating by ~1, 8, 20, and 70 μM DV, all in 1 mM AMP (E). (B–D) Inhibition of P_o by AMP (B), ADP (C), and ATP (D) in the presence of DV (8.4 ± 0.2 μM in B, 1.6 ± 0.05 μM in C and D). (F–H) Stimulation of P_o by DV in the presence of 1 mM AMP (F), ADP (G), and ATP (H). Solid lines are fits to the Hill equation (Eq. 1, MATERIALS AND METHODS), midpoints ($K_{1/2}$) are printed in the panels, Hill coefficients (n) were 0.7 ± 0.1 (B), 2.1 ± 0.5 (C), 0.9 ± 0.2 (D), 1.5 ± 0.5 (F), 1.8 ± 0.5 (G), 0.9 ± 0.4 (H). Replotted, as reference, are control dose response curves (empty symbols, dotted lines) in the absence of DV for B–D (from Fig. 1 B) and in the absence of nucleotides for F–H (from Fig. 5 B).

vated channels including high-affinity inhibition of opening rate and low-affinity stimulation of closing rate (Fig. 2, A and D–F). In particular, $K_{1/2}$ for inhibition of opening rate, a direct measure of ATP affinity of the closed channel (see below), was comparable for freshly excised channels (15 ± 2 μM) and deactivated ones (11 ± 2 μM). Thus, nucleotide inhibition is an intrinsic property of CA-NSC channels that is not altered during post-excision rundown.

Inhibition by Cytosolic Nucleotides Is Consistent with Simple Reversible Binding

We found that micromolar cytosolic nucleotides inhibited gating of CA-NSC channels by slowing opening rate and speeding closure. The higher apparent affinity for affecting opening rate than closing rate was consistent with a microscopically reversible four-state scheme (Fig. 1 E) in which nucleotides bind more tightly to the closed channel and therefore, in return, stabilize the closed state. We have previously reported that Ca^{2+} and voltage regulate channel gating in a complex fashion consistent with multiple open and closed states (Csanády and Adam-Vizi, 2003). How can our analysis based on the simple four-state model in Fig. 1 E be reconciled with those findings? The four states of the simple scheme have to be understood as compound states, e.g., the bottom-left state comprises all elementary states of the channel in which the pore is closed and the nucleotide binding site unliganded, regardless of the status of the Ca^{2+} binding site(s) and the voltage sensor(s). It is easy to show that the principle of microscopic reversibility holds up when applied to the average rates of transition among such compound states (see online supplemental material, section 1, Eq. 8, available at http://www.jgp.org/cgi/content/full/jgp.200309008/DC1). Although our average opening and closing rates, defined simply as the inverse of the arithmetic means of single-channel open and closed dwell-times and extracted from patches with multiple channels (see MATERIALS AND METHODS), are relatively simple measures of channel gating, their use in this study is justified by two arguments. First, extraction of these average parameters by the cycle-time method is robust and model independent. Second, the equations that predict opening and closing rates and P_o as a function of nucleotide concentration for the model in Fig. 1 E (online supplemental material, section 2.1, Eqs. 9, 10, and 12) are valid regardless of whether the 4 states in that scheme are simple ("elementary") states, or "compound" states composed themselves of sets of in-

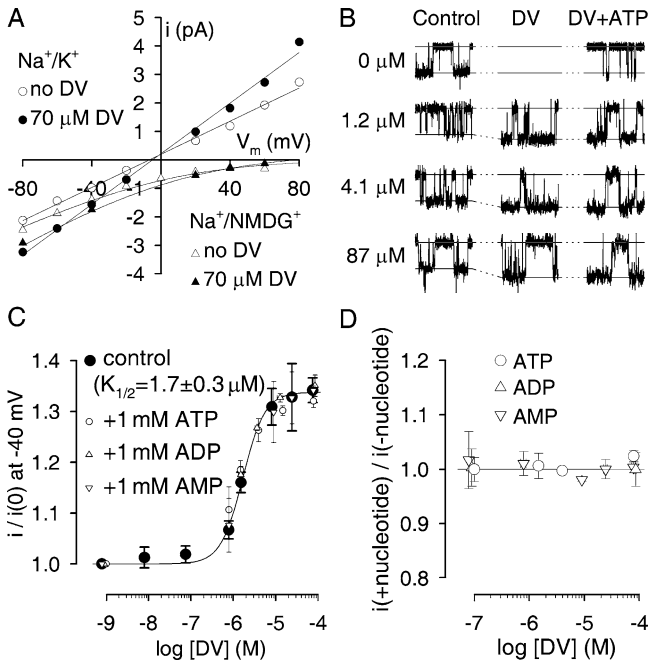

FIGURE 7. Stimulation of single-channel conductance by micromolar concentrations of DV. (A) Single-channel *i(V)* plots in the absence of (empty symbols), or in saturating (70 μM) DV (solid symbols). Pipette solution was 140 mM NaCl, bath solution was 140 mM of either KCl (circles and straight-line fits) or NMDG-Cl (triangles and fits to the Goldman-Hodgkin-Katz current equation). (B) Single-channel current sizes at −40 mV holding potential in the absence and presence of increasing [DV], or DV+ATP, normalized to that under control conditions in the same patch. (C) Normalized single-channel conductance as a function of cytosolic [DV] in the absence of nucleotides (control, black), or in the presence of 1 mM ATP, ADP, or AMP (empty symbols). Solid line is a fit to the Hill equation (Eq. 1, MATERIALS AND METHODS) for the control condition, $K_{1/2}$ is printed in the panel, $n = 1.7 \pm 0.4$. (D) Fractional change in single-channel conductance upon addition of 1 mM ATP, ADP, or AMP, in the presence of various [DV].

terconnected "elementary" states. (In the latter case, of course, the transition rates between states have to be taken as average rates of transition between compound states; for the "vertical" transitions in the scheme, these are exactly the average opening and closing rates we extract from our data using the cycle-time method.) Our study clearly shows that, using these simple parameters, the mechanism of the nucleotide and DV effects can be deciphered in the absence of a detailed understanding of the underlying Ca^{2+}- and voltage-dependent gating.

The Conformation of the Nucleotide Binding Site Senses the Conformation of the Gate, but Not of the Ca^{2+} and Voltage Sensors

The equilibrium between open and closed states of the CA-NSC channel (i.e., "vertical" transitions in Fig. 1 E) is regulated by $[Ca^{2+}]_i$ and voltage. In principle these parameters could also affect the equilibrium of the "horizontal" transitions in that scheme, i.e., nucleotide binding affinity of the closed, and/or open, channel, thereby altering apparent sensitivity to nucleotide inhibition. Indeed, a 10-fold elevation of $Ca^{2+}{}_i$ (to 10 mM, Fig. 2 B) resulted in an ~3-fold increase of $K_{1/2}$ for inhibition of P_o (K_{Po}) by ATP (Fig. 2 D), while hyperpolarization by −40 mV (to −80 mV) decreased that value by ~2-fold relative to control (Fig. 2, C and D), consistent with reports on CA-NSC channels in other tissues (Gray and Argent, 1990; Halonen and Nedergaard, 2002; Liman, 2003). However, while $K_{1/2}$ for inhibition of opening rate has a simple physical meaning, in that it is equal to the dissociation constant of the ligand from the closed channel (K_d^c, online supplemental material, section 2.1, Eq. 9), $K_{1/2}$ for inhibition of P_o (K_{Po}) is a more complicated parameter calculated as $K_{Po} = K_d^c (1 - P_1)/(1 - P_0)$, where P_0 and P_1 are open probabilities of unliganded and liganded channels, respectively (online supplemental material, section 2.1, Eq. 12). Because P_o of nucleotide-bound channels was small ($P_1 << 1$), the above equation can be simplified to $K_{Po} \approx K_d^c/(1 - P_0)$. Accordingly, at −40 mV in 1 mM $Ca^{2+}{}_i$, where P_0 was ~0.5, $K_{Po} \approx 2K_d^c$ is expected, as found for ATP, ADP, and AMP (compare Fig. 1 B and C). At −80 mV in 1 mM $Ca^{2+}{}_i$ P_0 was small (~0.2), therefore, K_{Po} is expected to be similar to K_d^c ($K_{Po} \approx 1.3K_d^c$), not inconsistent with that found for ATP (Fig. 2, D and E). Finally, at −40 mV in 10 mM $Ca^{2+}{}_i$, P_0 was ~0.8 (and $P_1 = 0.08$), therefore, $K_{Po} \approx 4.6K_d^c$ is expected, in good agreement with our ATP data (Fig. 2, D and E). (Indeed, the comparison holds up even for our tentative analysis on freshly excised channels in 100 μM Ca^{2+} [Fig. 2 A], for which average P_0 in bracketing control segments was ~0.6, and thus, $K_{Po} \approx 2.5K_d^c$ is expected.) Importantly, the measured K_d^c values for ATP were not significantly changed by a 10-fold increase in Ca^{2+} or a −40-mV change in voltage (Fig. 2 E). Thus, the apparent Ca^{2+} and voltage dependence of nucleotide inhibition of P_o (Fig. 2 D) simply reflects different P_o in the absence of nucleotide under those conditions. That is, Ca^{2+} and voltage alter the fraction of time the channel spends in the high-affinity closed state vs. the low-affinity open state, while ATP-affinity itself of (at least) the closed channel is not sensitive to Ca^{2+} and voltage. The conformation of the ATP binding site senses only whether the channel is closed or open, not the actual state of the Ca^{2+} and voltage sensors.

Nucleotide Sensitivity Profile Outlines a Subfamily of CA-NSC Channels

Ca^{2+}-activated monovalent cation-selective channels are present in several native tissues and differing nucleotide sensitivity profiles have been found for the ones

that were examined in detail. The CA-NSC channels present in astrocytes, for example, are clearly different from the brain endothelial channel, in that they are inhibited by ATP but are insensitive to ADP and AMP and have been suggested to be coupled to the type 1 sulphonylurea receptor (Chen et al., 2003). The order of inhibitory potency AMP > ADP > ATP >> Ado we found for the brain endothelial channel (Figs. 1 and 3) is similar to that reported for CA-NSC channels in the endocrine pancreas (Sturgess et al., 1986), in the kidney (Paulais and Teulon, 1989), and in brown fat cells (Halonen and Nedergaard, 2002), suggesting that these might form a unique subfamily of CA-NSC channels, even though subtle differences exist among them; e.g., cyclic nucleotides, which inhibit the CA-NSC of brown fat cells (Halonen and Nedergaard, 2002), failed to affect gating of the brain endothelial channel (Fig. 3). Interestingly, Ca^{2+} sensitivity (micromolar) of this latter subfamily of channels is also similar, while the astrocyte channel is activated by nanomolar Ca^{2+}.

At present it is not known which gene(s) encodes the native CA-NSC channels, and whether both their Ca^{2+} and nucleotide sensitivities are accounted for by a single polypeptide. Possible candidates include some members of the Trp ion channel family that form cation channels and require intracellular Ca^{2+} for gating. The Ca^{2+}-permeable TrpM2 is also nucleotide sensitive in that it is activated (unlike the brain endothelial CA-NSC, see Fig. 3 A) by cytosolic ADPribose and NAD^+, which bind to a COOH-terminal domain of the TrpM2 protein (Perraud et al., 2001; Sano et al., 2001). The closest functional matches to native CA-NSC channels are TrpM4b (Launay et al., 2002; Nilius et al., 2003) and TrpM5 (Hofmann et al., 2003; Liu and Liman, 2003; Prawitt et al., 2003), both ~25-pS, monovalent cation selective, Ca^{2+}- and voltage-activated channels. While nucleotide sensitivity has so far not been reported for TrpM5, in a recent report (Nilius et al., 2004) TrpM4b, expressed in HEK-293 cells, was shown to be inhibited by micromolar cytosolic adenine nucleotides, although some of the details were distinct from those described here for the brain endothelial CA-NSC channel; e.g., ~20% of TrpM4b current was insensitive to even millimolar [ATP], ADP was the most potent inhibitor, GTP and UTP were poor inhibitors, and it was concluded that free ATP is the species responsible for ATP inhibition.

Mutually Exclusive Binding Explains Antagonistic Regulation of Gating of CA-NSC Channels by Nucleotides and Decavanadate

DV stimulated gating with extremely high (nanomolar) affinity (Fig. 5). This tight binding of the highly charged DV molecule (6 negative charges) implies strong electrostatic interactions, which in turn suggests that positively charged arginine sidechains may contribute to its binding site (Soman et al., 1983; Toyoshima et al., 2000). The fact that DV, when added concomitantly, could similarly prevent inhibition by either ATP, ADP, or AMP, implicitly suggests that the latter three nucleotides all share a common binding site; unlike ATP-sensitive K^+ channels which possess distinct binding sites for inhibitory ATP (on the pore-forming Kir6.x channel subunit) and stimulatory MgADP (on the regulatory SUR subunit), but are insensitive to AMP, the most potent inhibitor of the CA-NSC channel.

DV also increased single-channel conductance by ~30% without grossly altering selectivity properties (Popp and Gögelein, 1992; Csanády and Adam-Vizi, 2003). This effect on the pore required micromolar [DV] (Figs. 5 A and 7 B) and was not influenced by the presence of nucleotides. We therefore conclude that DV affects the permeation properties of CA-NSC channels by binding with lower affinity to a site, presumably close to the pore, separate from the one at which it exerts its gating effect. Possibly, DV bound in the pore alters the local electrostatic potential so as to increase the local concentration of permeating cations, and hence the unitary conductance, as has been reported for both cation (MacKinnon et al., 1989; Nimigean et al., 2003) and anion channels (Middleton et al., 1996; Chen and Chen, 2003). A detailed study should be undertaken to address this issue for the CA-NSC channel.

Setting aside this affect on permeation, all our observations on channel gating in the presence of ATP, ADP, AMP, and DV, including changes in P_o as well as gating kinetics, are easily explained by extending the model in Fig. 1 E (cartoon in Fig. 8). A single site on the cytosolic face of the CA-NSC channel which binds either ATP, ADP, or AMP undergoes an obligate conformational change upon channel opening (and closure). Nucleotides bind tightly (micromolar K_d) in the closed, but only loosely (millimolar K_d) in the open, channel conformation, thereby stabilizing the closed state (Fig. 1, C–E). DV binds competitively to the same site, but is bound more tightly in the open (nanomolar K_d) than in the closed state (micromolar K_d), thereby stabilizing the open-channel conformation. The graphs in Fig. 8 replot the 18 dose response curves of steady-state P_o, opening, and closing rates from Figs. 1, 5, and 6. Whereas in the above figures these plots were individually fitted with the Hill equation, the bold lines in Fig. 8 (and predicted $K_{1/2}$ values in each graph; derived in online supplemental material, section 2.1, Eqs. 9, 10, and 12, and section 2.2, Eq. 14b) result from a simultaneous fit of the cartooned gating model to the ensemble of all 18 curves. With only nine adjustable parameters (gray boxes), the good overall fit to all 18 curves supports this simple model. (Opening rate of the unliganded channel was fixed to its average value, white

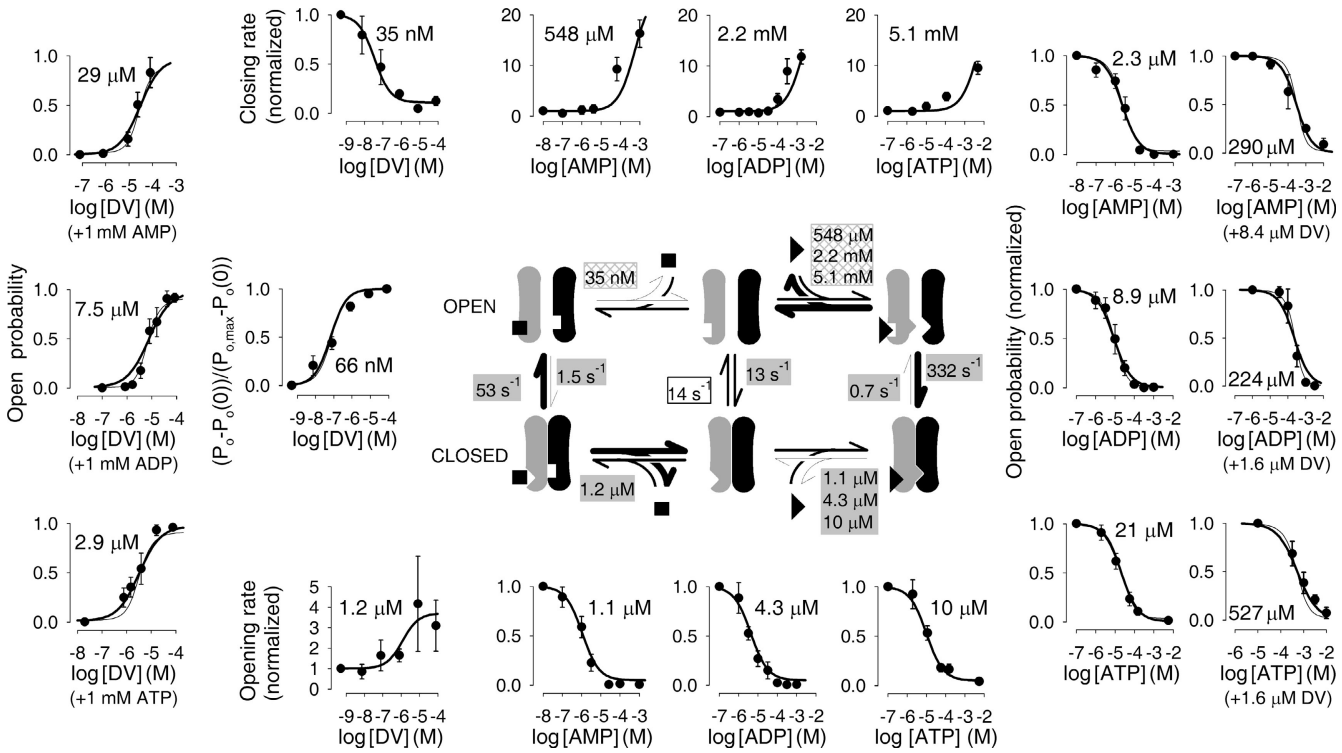

FIGURE 8. Competitive binding of DV and nucleotides to a single site quantitatively accounts for all the data. (Scheme, center) The binding site changes conformation upon channel opening. Nucleotides (triangles) bind more tightly in the closed conformation, therefore, binding of these ligands stabilizes the closed state. DV (square) binds more tightly to the open conformation, thereby stabilizing the open state. Dose response curves are replotted from Figs. 1, B–D; 5, B–D; and 6, B–D and F–H. Bold lines are the results of a nine free parameter ensemble fit of the cartooned model to all 18 dose response curves. Free parameters (gray boxes) were closing rate of unliganded channels, opening and closing rates of nucleotide- and DV-bound channels, as well as K_ds of closed channels for ATP, ADP, AMP, and DV. K_ds of open channels for these ligands (checked boxes) were constrained by microscopic reversibility, opening rate of unliganded channels (white box) was fixed to its average value (at −40 mV in 1 mM Ca^{2+}_i). The numbers on the model are the obtained fit parameters, the numbers in the plots are midpoints (i.e., half-maximally efficient ligand concentrations) for each curve predicted by the fit parameters shown in the center. Thin lines in P_o-plots are fits of those plots to a model with four independent subunits, each described by the scheme in the center.

box; K_ds for ligand binding of open channels are constrained by microscopic reversibility, checked boxes.)

We have also considered the alternative à priori possibility, namely that ATP and DV bind to separate sites (noncompetitive model; the kinetic treatment of this model can be found in section 2.3 of the online supplemental material). Such a model with independent binding sites for nucleotides and DV did not fit our data. If binding of DV was allowed to allosterically destabilize the nucleotide binding site (in which case, by microscopic reversibility, nucleotide binding must destabilize the DV binding site), our data could be fitted, but predicted huge decreases in nucleotide affinity brought upon by DV binding (∼200-, 10^5-, and 10^3-fold for ATP, ADP, and AMP). This would mean that simultaneous binding of nucleotide and DV would almost never occur, i.e., from a kinetic point of view, the model reduces to the mutually exclusive model (competitive binding), which is a subset of the more general model (allowing simultaneous binding). E.g., the fits for ADP suggest that even when both [ADP] and [DV] are 1,000× their own $K_{1/2}$, the channel spends 99.5% of its time without both ligands simultaneously bound.

While we could reasonably fit our data assuming one ATP binding site (Fig. 8), most cation channels are multimeric; Trp channels, for example, are believed to function as tetramers (Harteneck et al., 2000). Therefore, even if the CA-NSC channel is a heteromultimer, it is plausible to expect more than one ATP binding site (possibly 2, 3, or 4) per channel molecule. Our data did not imply any significant cooperativity (Hill coefficients of most dose response curves were close to 1, the random scatter in the slopes of some of the curves, e.g., in Fig. 6, most likely reflect the stochastic nature of our single-channel data), but could be equally well fitted assuming 1–4 independent subunits with nucleotides and DV competing at each site (thin lines in the P_o plots of Fig. 8 show the fit for four subunits; see kinetic treat-

ment in section 2.4. of the online supplemental material). Fitting of models with 2–4 independent subunits each containing separate binding sites for nucleotides and DV (compare online supplemental material, section 2.5) still required strong negative allosteric interaction, although the extent of mutual destabilization required for a good fit decreased with the number of assumed subunits (~50–70-fold for $n = 4$). A scheme assuming four binding sites for ATP and a single separate allosteric binding site for DV (modeled on the binding of 2,3-bisphosphoglycerate and O_2 to hemoglobin; Benesch and Benesch, 1969; see online supplemental material, section 2.6) could not be adequately fitted to our data. (See fits to various models in section 3 [Fig. S1] of the online supplemental material.)

Among the proteins known to interact with DV, several contain nucleotide binding sites, including the sulphonylurea-receptor subunits of ATP-sensitive K^+ channels (Proks et al., 1999). For most of these enzymes the exact site of binding of DV relative to that of the nucleotides was not addressed (Boyd et al., 1985; Proks et al., 1999) or was inferred simply from the competitive (Menon and Goldberg, 1987; Krivanek, 1994) or noncompetitive (Choate and Mansour, 1979; Soman et al., 1983; Pezza et al., 2002) kinetic patterns. However, x-ray crystallographic data for adenylate kinase (Pai et al., 1977) and combined evidence from biochemical (Csermely et al., 1985; Coan et al., 1986; Ross and McIntosh, 1987; Hua et al., 2000) and crystallographic (Toyoshima et al., 2000) data for the sarcoplasmic Ca^{2+}-ATPase have unambiguously confirmed that DV binds at the nucleotide binding site in these two proteins.

In summary, we conclude that ATP, ADP, and AMP inhibit by binding to a common site. Our data are consistent with 1–4 independent channel subunits, and indicate mutually exclusive binding of nucleotides and DV. While a strong negative allosteric interaction between separate nucleotide and DV sites is formally consistent with our data per se, the comparatively good fit with the simpler competitive model (Fig. 8) and the known binding of DV to nucleotide binding sites (Pai et al., 1977; Toyoshima et al., 2000) argue in favor of the latter explanation. A similar strategy of antagonistic regulation by two ligands binding competitively at the same site is employed by the enzyme ribonucleotide reductase, which is activated when ATP, but inhibited when dATP, binds to its primary regulatory site (Reichard et al., 2000).

Significance of Our Findings

The significance of our decavanadate results is twofold. First, decavanadate is the only high-affinity activator for CA-NSC channels known so far, and it provides a powerful new tool for future studies on these channels. In excised patch recordings, for example, maximal stimulation by micromolar decavanadate can be used to determine the number of active channels. Furthermore, as the exact molecular identity of the CA-NSC channels is still unknown, decavanadate stimulation provides a new functional fingerprint that can be used to screen heterologously expressed cloned channels. Second, the fact that decavanadate allows channels to gate in the presence of millimolar cytosolic nucleotides suggests a possible explanation for how cytosolic Ca^{2+} signals (Maruyama and Petersen, 1982; Kamouchi et al., 1999; Koivisto et al., 2000) can activate CA-NSC channels in living cells. Binding of some negatively charged metabolite to the decavanadate binding site (regardless of its location) could provide a simple way for the cell to regulate the readiness of CA-NSC channels to respond to rises in cytosolic Ca^{2+} in the presence of millimolar nucleotides. Future studies will have to identify any such natural activating ligand of the CA-NSC channel.

We thank Dr. David Gadsby for valuable discussions and critical reading of the manuscript, and Katalin Takács for preparation of brain endothelial cells.

Supported by grants from OTKA, ETT, and MTA to V. Adam-Vizi.

Olaf S. Andersen served as editor.

Submitted: 30 December 2003
Accepted: 6 May 2004

REFERENCES

Benesch, R., and R.E. Benesch. 1969. Intracellular organic phosphates as regulators of oxygen release by haemoglobin. *Nature.* 221:618–622.

Boyd, D.W., K. Kustin, and M. Niwa. 1985. Do vanadate polyanions inhibit phosphotransferase enzymes? *Biochim. Biophys. Acta.* 827: 472–475.

Caceci, M.S., and W.P. Cacheris. 1984. Fitting curves to data. The simplex algorithm is the answer. *Byte.* May:340–348.

Chen, M., Y. Dong, and J.M. Simard. 2003. Functional coupling between sulfonylurea receptor type 1 and a nonselective cation channel in reactive astrocytes from adult rat brain. *J. Neurosci.* 23: 8568–8577.

Chen, M., and J.M. Simard. 2001. Cell swelling and a nonselective cation channel regulated by internal Ca^{2+} and ATP in native reactive astrocytes from adult rat brain. *J. Neurosci.* 21:6512–6521.

Chen, M.F., and T.Y. Chen. 2003. Side-chain charge effects and conductance determinants in the pore of ClC-0 chloride channels. *J. Gen. Physiol.* 122:133–145.

Choate, G., and T.E. Mansour. 1979. Studies on heart phosphofructokinase. Decavanadate as a potent allosteric inhibitor at alkaline and acidic pH. *J. Biol. Chem.* 254:11457–11462.

Coan, C., D.J. Scales, and A.J. Murphy. 1986. Oligovanadate binding to sarcoplasmic reticulum ATPase. Evidence for substrate analogue behavior. *J. Biol. Chem.* 261:10394–10403.

Colquhoun, D., E. Neher, H. Reuter, and C.F. Stevens. 1981. Inward current channels activated by intracellular Ca in cultured cardiac cells. *Nature.* 294:752–754.

Csanády, L. 2000. Rapid kinetic analysis of multichannel records by a simultaneous fit to all dwell-time histograms. *Biophys. J.* 78:785–799.

Csanády, L., and V. Adam-Vizi. 2003. Ca^{2+}- and voltage-dependent gating of Ca^{2+}- and ATP-sensitive cationic channels in brain capillary endothelium. *Biophys. J.* 85:313–327.

Csanády, L., K.W. Chan, D. Seto-Young, D.C. Kopsco, A.C. Nairn, and D.C. Gadsby. 2000. Severed channels probe regulation of gating of cystic fibrosis transmembrane conductance regulator by its cytoplasmic domains. *J. Gen. Physiol.* 116:477–500.

Csermely, P., S. Varga, and A. Martonosi. 1985. Competition between decavanadate and fluorescein isothiocyanate on the Ca^{2+}-ATPase of sarcoplasmic reticulum. *Eur. J. Biochem.* 150:455–460.

Dömötör, E., I. Sipos, A. Kittel, N.J. Abbott, and V. Adam-Vizi. 1998. Improved growth of cultured brain microvascular endothelial cells on glass coated with a biological matrix. *Neurochem. Int.* 33: 473–478.

Gögelein, H., and K. Capek. 1990. Quinine inhibits chloride and nonselective cation channels in isolated rat distal colon cells. *Biochim. Biophys. Acta.* 1027:191–198.

Gray, M.A., and B.E. Argent. 1990. Non-selective cation channel on pancreatic duct cells. *Biochim. Biophys. Acta.* 1029:33–42.

Guinamard, R., M. Rahmati, J. Lenfant, and P. Bois. 2002. Characterization of a Ca^{2+}-activated nonselective cation channel during dedifferentiation of cultured rat ventricular cardiomyocytes. *J. Membr. Biol.* 188:127–135.

Halonen, J., and J. Nedergaard. 2002. Adenosine 5′-monophosphate is a selective inhibitor of the brown adipocyte nonselective cation channel. *J. Membr. Biol.* 188:183–197.

Harteneck, C., T.D. Plant, and G. Schultz. 2000. From worm to man: three subfamilies of TRP channels. *Trends Neurosci.* 23:159–166.

Hofmann, T., V. Chubanov, T. Gudermann, and C. Montell. 2003. TRPM5 is a voltage-modulated and Ca^{2+}-activated monovalent selective cation channel. *Curr. Biol.* 13:1153–1158.

Hua, S., G. Inesi, and C. Toyoshima. 2000. Distinct topologies of mono- and decavanadate binding and photo-oxidative cleavage in the sarcoplasmic reticulum ATPase. *J. Biol. Chem.* 275:30546–30550.

Jung, F., S. Selvaraj, and J.J. Gargus. 1992. Blockers of platelet-derived growth factor-activated nonselective cation channel inhibit cell proliferation. *Am. J. Physiol.* 262:C1464–C1470.

Kamouchi, M., A. Mamin, G. Droogmans, and B. Nilius. 1999. Nonselective cation channels in endothelial cells derived from human umbilical vein. *J. Membr. Biol.* 169:29–38.

Koivisto, A., D. Siemen, and J. Nedergaard. 2000. Norepinephrine-induced sustained inward current in brown fat cells: α(1)-mediated by nonselective cation channels. *Am. J. Physiol. Endocrinol. Metab.* 279:E963–E977.

Krivanek, J. 1994. Effect of vanadium ions on ATP citrate lyase. *Gen. Physiol. Biophys.* 13:43–55.

Launay, P., A. Fleig, A.L. Perraud, A.M. Scharenberg, R. Penner, and J.P. Kinet. 2002. TRPM4 is a Ca^{2+}-activated nonselective cation channel mediating cell membrane depolarization. *Cell.* 109: 397–407.

Liman, E.R. 2003. Regulation by voltage and adenine nucleotides of a Ca^{2+}-activated cation channel from hamster vomeronasal sensory neurons. *J. Physiol.* 548:777–787.

Liu, D., and E.R. Liman. 2003. Intracellular Ca^{2+} and the phospholipid PIP2 regulate the taste transduction ion channel TRPM5. *Proc. Natl. Acad. Sci. USA.* 100:15160–15165.

Loussouarn, G., L.J. Pike, F.M. Ashcroft, E.N. Makhina, and C.G. Nichols. 2001. Dynamic sensitivity of ATP-sensitive K^+ channels to ATP. *J. Biol. Chem.* 276:29098–29103.

MacGregor, G.G., K. Dong, C.G. Vanoye, L. Tang, G. Giebisch, and S.C. Hebert. 2002. Nucleotides and phospholipids compete for binding to the C terminus of KATP channels. *Proc. Natl. Acad. Sci. USA.* 99:2726–2731.

MacKinnon, R., R. Latorre, and C. Miller. 1989. Role of surface electrostatics in the operation of a high-conductance Ca^{2+}-activated K^+ channel. *Biochemistry.* 28:8092–8099.

Marty, A., Y.P. Tan, and A. Trautmann. 1984. Three types of calcium-dependent channel in rat lacrimal glands. *J. Physiol.* 357: 293–325.

Maruyama, Y., and O.H. Petersen. 1982. Cholecystokinin activation of single-channel currents is mediated by internal messenger in pancreatic acinar cells. *Nature.* 300:61–63.

Menon, A.S., and A.L. Goldberg. 1987. Binding of nucleotides to the ATP-dependent protease La from *Escherichia coli. J. Biol. Chem.* 262:14921–14928.

Middleton, R.E., D.J. Pheasant, and C. Miller. 1996. Homodimeric architecture of a ClC-type chloride ion channel. *Nature.* 383:337–340.

Nilius, B., J. Prenen, G. Droogmans, T. Voets, R. Vennekens, M. Freichel, U. Wissenbach, and V. Flockerzi. 2003. Voltage dependence of the Ca^{2+}-activated cation channel TRPM4. *J. Biol. Chem.* 278: 30813–30820.

Nilius, B., J. Prenen, T. Voets, and G. Droogmans. 2004. Intracellular nucleotides and polyamines inhibit the Ca^{2+}-activated cation channel TRPM4b. *Pflugers Arch.* 448:70–75.

Nimigean, C.M., J.S. Chappie, and C. Miller. 2003. Electrostatic tuning of ion conductance in potassium channels. *Biochemistry.* 42:9263–9268.

Pai, E.F., W. Sachsenheimer, R.H. Schirmer, and G.E. Schulz. 1977. Substrate positions and induced-fit in crystalline adenylate kinase. *J. Mol. Biol.* 114:37–45.

Paulais, M., and J. Teulon. 1989. A cation channel in the thick ascending limb of Henle's loop of the mouse kidney: inhibition by adenine nucleotides. *J. Physiol.* 413:315–327.

Pérez, G.J., A.D. Bonev, and M.T. Nelson. 2001. Micromolar Ca^{2+} from sparks activates Ca^{2+}-sensitive K^+ channels in rat cerebral artery smooth muscle. *Am. J. Physiol. Cell Physiol.* 281:C1769–C1775.

Perraud, A.L., A. Fleig, C.A. Dunn, L.A. Bagley, P. Launay, C. Schmitz, A.J. Stokes, Q. Zhu, M.J. Bessman, R. Penner, et al. 2001. ADP-ribose gating of the calcium-permeable LTRPC2 channel revealed by Nudix motif homology. *Nature.* 411:595–599.

Petersen, O.H. 2002. Cation channels: homing in on the elusive CAN channels. *Curr. Biol.* 12:R520–R522.

Pezza, R.J., M.A. Villarreal, G.G. Montich, and C.E. Argarana. 2002. Vanadate inhibits the ATPase activity and DNA binding capability of bacterial MutS. A structural model for the vanadate-MutS interaction at the Walker A motif. *Nucleic Acids Res.* 30:4700–4708.

Popp, R., and H. Gögelein. 1992. A calcium and ATP sensitive nonselective cation channel in the antiluminal membrane of rat cerebral capillary endothelial cells. *Biochim. Biophys. Acta.* 1108:59–66.

Prawitt, D., M.K. Monteilh-Zoller, L. Brixel, C. Spangenberg, B. Zabel, A. Fleig, and R. Penner. 2003. TRPM5 is a transient Ca^{2+}-activated cation channel responding to rapid changes in $[Ca^{2+}]i$. *Proc. Natl. Acad. Sci. USA.* 100:15166–15171.

Prescott, E.D., and D. Julius. 2003. A modular PIP2 binding site as a determinant of capsaicin receptor sensitivity. *Science.* 300:1284–1288.

Proks, P., R. Ashfield, and F.M. Ashcroft. 1999. Interaction of vanadate with the cloned beta cell K(ATP) channel. *J. Biol. Chem.* 274: 25393–25397.

Reichard, P., R. Eliasson, R. Ingemarson, and L. Thelander. 2000. Cross-talk between the allosteric effector-binding sites in mouse ribonucleotide reductase. *J. Biol. Chem.* 275:33021–33026.

Rohacs, T., C.M. Lopes, T. Jin, P.P. Ramdya, Z. Molnar, and D.E. Logothetis. 2003. Specificity of activation by phosphoinositides determines lipid regulation of Kir channels. *Proc. Natl. Acad. Sci.*

USA. 100:745–750.

Ross, D.C., and D.B. McIntosh. 1987. Intramolecular cross-linking at the active site of the Ca^{2+}-ATPase of sarcoplasmic reticulum. High and low affinity nucleotide binding and evidence of active site closure in E2-P. *J. Biol. Chem*. 262:12977–12983.

Sano, Y., K. Inamura, A. Miyake, S. Mochizuki, H. Yokoi, H. Matsushime, and K. Furuichi. 2001. Immunocyte Ca^{2+} influx system mediated by LTRPC2. *Science*. 293:1327–1330.

Soman, G., Y.C. Chang, and D.J. Graves. 1983. Effect of oxyanions of the early transition metals on rabbit skeletal muscle phosphorylase. *Biochemistry*. 22:4994–5000.

Sturgess, N.C., C.N. Hales, and M.L. Ashford. 1986. Inhibition of a calcium-activated, non-selective cation channel, in a rat insulinoma cell line, by adenine derivatives. *FEBS Lett*. 208:397–400.

Suh, S.H., H. Watanabe, G. Droogmans, and B. Nilius. 2002. ATP and nitric oxide modulate a Ca^{2+}-activated non-selective cation current in macrovascular endothelial cells. *Pflugers Arch*. 444: 438–445.

Suzuki, K., and O.H. Petersen. 1988. Patch-clamp study of single-channel and whole-cell K^+ currents in guinea pig pancreatic acinar cells. *Am. J. Physiol*. 255:G275–G285.

Toyoshima, C., M. Nakasako, H. Nomura, and H. Ogawa. 2000. Crystal structure of the calcium pump of sarcoplasmic reticulum at 2.6 A resolution. *Nature*. 405:647–655.

Tucker, S.J., and F.M. Ashcroft. 1998. A touching case of channel regulation: the ATP-sensitive K^+ channel. *Curr. Opin. Neurobiol*. 8:316–320.

Varga, S., P. Csermely, and A. Martonosi. 1985. The binding of vanadium (V) oligoanions to sarcoplasmic reticulum. *Eur. J. Biochem*. 148:119–126.

Yellen, G. 1982. Single Ca^{2+}-activated nonselective cation channels in neuroblastoma. *Nature*. 296:357–359.